Article

Not peer-reviewed version

Process Control and Intensification with Hydrodynamic Cavitation: Architectures and Design Space of a Dynamic Circular Venturi

Lorenzo Albanese *

Posted Date: 24 February 2026

doi: 10.20944/preprints202602.1423.v1

Keywords: hydrodynamic cavitation; venturi reactor; system design; reconfigurable geometry

doi:10.20944/preprints202602.1423.v1

Article

Process Control and Intensification with Hydrodynamic Cavitation: Architectures and Design Space of a Dynamic Circular Venturi

Lorenzo Albanese

Institute of Bioeconomy, National Research Council of Italy, Via Madonna del Piano 10, 50019 Florence, Italy; lorenzo.albanese@cnr.it

Abstract

Hydrodynamic cavitation in process plants is often generated by static devices designed for nominal operating conditions. In real processes, however, the properties of the process fluid, including temperature, viscosity, and gas and solids content, may vary. Consequently, maintaining the cavitation regime within a target operating window over extended periods is challenging. The Dynamic Circular Venturi (DCVA) is introduced as a circular Venturi with an internal geometry that can be reconfigured during operation. The external body and connections are preserved, while the internal configuration, particularly the throat section, can be adjusted. A formalism based on equivalent geometric parameters is proposed to describe the set of admissible configurations. A dedicated design space is also defined to identify, for a given architecture, the subset that is practically accessible. Two implementations are presented: a single degree-of-freedom layout for throat-opening modulation and a multiparametric layout based on axial stations, enabling the generation of a family of internal profiles. An estimated operating indicator is introduced and formulated using variables typically measured in process plants, supporting configuration selection and the specification of operating settings. This conceptual framework can support the optimization of sustainable food-processing operations enabled by hydrodynamic cavitation, such as green extraction and food by-product valorization, with potential gains in resource efficiency and waste minimization.

Keywords: hydrodynamic cavitation; venturi reactor; system design; reconfigurable geometry

---

1. Introduction

In industrial practice, hydrodynamic cavitation is typically achieved using static devices designed for a specific operating point, most commonly circular-throat Venturi devices. In real processes, however, the processed medium evolves over time due to variations in temperature, viscosity, and gas and solids content, while the device geometry remains unchanged. Consequently, the optimal operating regime is difficult to maintain over extended periods.

Hydrodynamic cavitation is widely used in industry as a process-intensification technology and has recently attracted increasing interest in food processing and other green applications. It has also been applied to plant- and biomass-based extraction and valorisation. Moreover, water-treatment applications have been reported using dedicated hydrodynamic cavitation generators.

In this context, controlled hydrodynamic cavitation generally refers to the regulation of operating conditions and the use of plant-measurable variables to improve repeatability and robustness, without modifying the installed cavitation device.

Concurrently, many studies on cavitating Venturi devices focus on geometric design and optimization as well as the characterization of cavitating flow, while typically assuming a configuration defined at the design stage and then kept constant during operation. In other fields, variable-geometry Venturi devices have been developed, such as variable-throat Venturi scrubbers, to modulate pressure drop and collection efficiency. Their objective, however, differs from maintaining a cavitation regime within a target operating window for processing and treatment applications.

Several studies have also examined variable-area cavitating Venturi devices as regulation and control elements, for example as dynamic flow controllers or within feedback control schemes, in application domains different from that considered here. In this context, it remains relevant from a plant perspective to formalize and design a reconfigurable cavitating Venturi that preserves in-line integration by keeping the external interfaces unchanged, while making the internal geometry an operating variable for stabilizing and positioning the cavitation regime with respect to a defined process target.

Within the broader field of hydrodynamic cavitation reactors, recent reviews highlight that reactor design, and particularly the constriction element design, plays a central role in determining cavitation mechanisms and process applicability in intensification scenarios.

Moreover, small cavitating Venturi devices have been investigated as in-line components, with experimental and numerical characterizations including cryogenic systems, providing a direct framing of Venturi-based cavitation generators beyond conventional flow-control applications.

In practice, the most effective cavitation operating point is often identified during commissioning, because process response depends on the actual feed properties and plant constraints and is assessed against performance targets such as extraction yield, selectivity, purity, or minimal degradation.

A Dynamic Circular Venturi (DCVA) supports this screening phase by enabling a structured sweep of throat opening and operating conditions to build commissioning maps and select a robust operating point, which can then be locked for single-product operation or retained as an in-line adjustment variable to preserve performance under variability.

The DCVA is proposed as a circular Venturi whose internal geometry can be reconfigured as an operating degree of freedom. The external body and plant interfaces remain unchanged, whereas the effective throat area can be adjusted during operation to enable hydrodynamic cavitation regime modulation without structural modifications to the plant. The set of achievable configurations is described through a formalism based on equivalent geometric parameters and a dedicated design space. The proposed framework supports consistent comparisons across different implementations and explicitly distinguishes the admissible configuration set from the subset that is practically accessible, depending on the selected device architecture.

The contribution of this work is twofold. First, two representative DCVA architectures are introduced at the conceptual system-design level, namely DCVA-S, a single degree-of-freedom configuration where the throat opening is an operating variable, and DCVA-M, a multiparametric configuration where multiple axial stations reconfigure the internal profile to generate a family of geometries. Second, an operational proxy indicator is introduced, formulated from quantities typically measurable in process plants, to support configuration selection and unambiguous specification of operating settings when local throat pressure is not available. The indicator is presented as a design-oriented surrogate rather than a validated replacement of the cavitation number, and no experimental campaign or high-fidelity CFD results are reported in this conceptual study.

2. DCVA Framework

A circular Venturi with a variable internal geometry is considered as a hydrodynamic cavitation module for processing complex liquid systems. The key feature of the concept is the ability to modify the internal geometry during operation, thereby adapting the cavitation regime to the properties of the treated medium and to the process target, without being constrained by a fixed geometry sized for a single operating point.

Overall, the DCVA is designed for in-line installation as a drop-in replacement for a conventional Venturi. The external body and plant interfaces, including diameters and connections,

Preprints.org (www.preprints.org) | NOT PEER-REVIEWED | Posted: 24 February 2026 doi:10.20944/preprints202602.1423.v1

remain unchanged, whereas the effective internal configuration, particularly at the throat, becomes an operating variable. This section defines the common quantities used to describe geometric reconfiguration and the cavitation regime.

2.1. Geometry and Control

Two characteristic throat diameters are defined. The minimum throat diameter, d, corresponds to the most constricted configuration and to a more intense cavitation regime. The maximum throat diameter, D, corresponds to the most open configuration and to a more moderate cavitation regime. Let $d_e(t)$ denote the equivalent throat diameter during operation. By construction:

$$d \le d_e(t) \le D \tag{1}$$

The interval $[d, D]$ represents the available geometric stroke. The ratio D/d quantifies the maximum relative opening achievable for a given external envelope. The minimum value d is set by process requirements, whereas D is limited by design constraints, including mechanical integrity, materials, and reliability, as well as by operating conditions.

To describe and control the throat opening, a dimensionless control variable is introduced:

$$\chi(t) = \frac{d_e(t) - d}{D - d}, \qquad 0 \le \chi(t) \le 1 \tag{2}$$

The value $\chi = 0$ corresponds to the minimum-throat configuration, $d_e(t) = d$, whereas $\chi = 1$ corresponds to the maximum-throat configuration, $d_e(t) = D$. Equation (2) yields the direct control-to-geometry relation:

$$d_e(t) = d + \chi(t)\,(D - d) \tag{3}$$

For clarity, the key parameters used to describe the DCVA architectures within the present framework are summarized in Table 1.

Table 1. Key parameters used to describe DCVA architectures within the present framework.

DCVA	DCVA-S	DCVA-M
d	χ	N
D	N_θ	x_i
d_e		u_i
L_t		
α_{in}		
α_{out}		

Note: In DCVA-S the geometry state d_e is controlled by χ, whereas in DCVA-M it is controlled by the station commands u_i; the station layout is defined by the axial locations x_i.

Within the DCVA framework, equivalent geometric parameters are also introduced to describe the shape of the internal profile. L_t denotes the equivalent length of the throat region, intended as the axial extent of the section close to the minimum. α_{in} and α_{out} denote the effective convergence and divergence angles, interpreted as equivalent slopes of the transition sections. Depending on the internal architecture, these parameters may be fixed by design or vary as a result of the kinematics. In both cases, they provide a compact description of the internal geometry and its hydrodynamic effects.

2.2. Hydrodynamics and Design Space

The cavitation regime can be characterized by a throat-based cavitation number. Let p_g denote the mean static pressure at the throat, v_g the mean velocity at the throat, $p_v\,(T)$ the vapor pressure at temperature T, and ρ the fluid density. The following definition is adopted:

$$\sigma = \frac{p_g - p_v(T)}{\frac{1}{2}\rho\, v_g^2} \tag{4}$$

In the following, all pressures are absolute (referenced to vacuum). In particular, p_{in}, p_{out}, p_g, and $p_v\,(T)$ are expressed as absolute values.

For given upstream and downstream plant conditions, varying the equivalent throat diameter d_e changes the throat velocity and shifts σ within the cavitation window of interest.

To represent admissible DCVA geometric configurations in a unified manner, a design space Ω is introduced.

$$\Omega \;=\; \left\{ (d_e,\, L_t,\, \alpha_{in},\, \alpha_{out}) \;\middle|\; \begin{array}{c} d \le d_e \le D \\ L_{t,min} \le L_t \le L_{t,max} \\ \alpha_{in,min} \le \alpha_{in} \le \alpha_{in,max} \\ \alpha_{out,min} \le \alpha_{out} \le \alpha_{out,max} \end{array} \right\} \tag{5}$$

In Equation (5), the "min" and "max" limits reflect mechanical and process constraints. The design space Ω therefore delineates the full set of admissible geometric configurations. The subset that is practically reachable, however, depends on the selected architecture and kinematic mechanism, which determine which parameters are directly controllable and which are instead fixed or coupled as induced effects.

2.3. Measured Signals and Indicator

In a process-plant context, a direct measurement of the throat pressure p_g may not be available. An online indicator is therefore introduced and computed from quantities typically measured in process plants, namely the inlet pressure p_{in}, the outlet pressure p_{out}, the volumetric flow rate Q, and the temperature T, from which $p_v(T)$ is obtained. The dependence on geometry is captured through the equivalent throat diameter d_e, computed from Equation (3) in the single-parameter case or derived from the equivalent profile in the multiparametric case.

A continuity-based estimate of the mean throat velocity, v_t, is adopted:

$$v_t = \frac{4Q}{\pi\, d_e^2} \tag{6}$$

Using v_t and plant-measurable quantities, the following operational indicator is defined:

$$\hat{\sigma} = \frac{p_{in} - p_v(T)}{\frac{1}{2}\, p\, v_t^2} \tag{7}$$

In the following, $\hat{\sigma}$ is used as an operational proxy for the cavitation regime, since it is computed from p_{in} and the equivalent throat diameter d_e through the velocity estimate v_t. Consequently, $\hat{\sigma}$ does not necessarily coincide with the local cavitation number σ in Equation (4), which would require a direct measurement of the throat pressure p_g. Here, subscript g denotes throat quantities. Accordingly, $\hat{\sigma}$ is introduced as a design-oriented proxy for consistent configuration selection and reporting, not as a validated replacement of σ.
A first-order deviation can be expressed by writing $p_g = p_{in} - \Delta p_{in\to g}$, where $\Delta p_{in\to g}$ accounts for inlet-to-throat losses. Under this definition, $\sigma = \hat{\sigma} - \Delta p_{in\to g}/(\frac{1}{2}\rho v_t^2)$; hence the deviation is governed by $\Delta p_{in\to g}$ and is quantified during commissioning for the specific duty.
Related validation studies highlight practical limits when using simplified indicators to represent cavitation intensity. When needed, non-idealities can be addressed through a calibrated flow coefficient for variable-area cavitating Venturi devices. The indicator $\hat{\sigma}$ is employed to build commissioning maps and to compare configurations in a repeatable manner under a consistent

 doi:10.20944/preprints202602.1423.v1

estimation criterion. The outlet pressure p_{out} is used to monitor operating conditions and, when needed, to verify plant constraints through the pressure drop $\Delta p = p_{in} - p_{out}$.

3. DCVA-S: Single-Parameter

The DCVA-S configuration implements a dynamic circular Venturi with a single actuated geometric degree of freedom, associated with the throat opening. The objective is to modulate the cavitation regime by acting on the internal Venturi geometry while keeping the inlet and outlet piping interfaces unchanged, thereby enabling in-line integration without modifications to the external piping.

3.1. Architecture Single

The DCVA-S consists of an outer cartridge and an internal system that reconfigures the wetted flow surface. In the figures, three functional subassemblies are highlighted and color-coded.

Blue pistons, external actuation: actuators arranged radially around the cartridge, synchronously actuated and described by a single control parameter χ.

White/gray pistons, kinematic cage: a movable internal cage guided within the cartridge, which transfers the displacement to the liner retaining elements. The cage is obtained by circumferential repetition of elementary modules.

Red liner, elastomer: a single-piece elastomeric component that forms the internal wetted surface. It is constrained by rings fixed to the cylinder bodies, the stationary part of the white/gray pistons, rather than to the moving rods, thereby reducing shear and lateral loads during reconfiguration.

Liner material selection and sizing are application-dependent and are therefore not prescribed in this sector-agnostic conceptual framework. The liner can be parameterized by thickness and effective stiffness, and the throat diameter variation can be expressed as a function of the liner radial deformation, to be specialized by implementers for their specific process constraints.

The throat section has a constant axial length, L_t, set by design and intended as the equivalent length of the throat region. During operation, the equivalent throat diameter d_e varies, whereas L_t is kept constant by kinematic mechanical constraints.

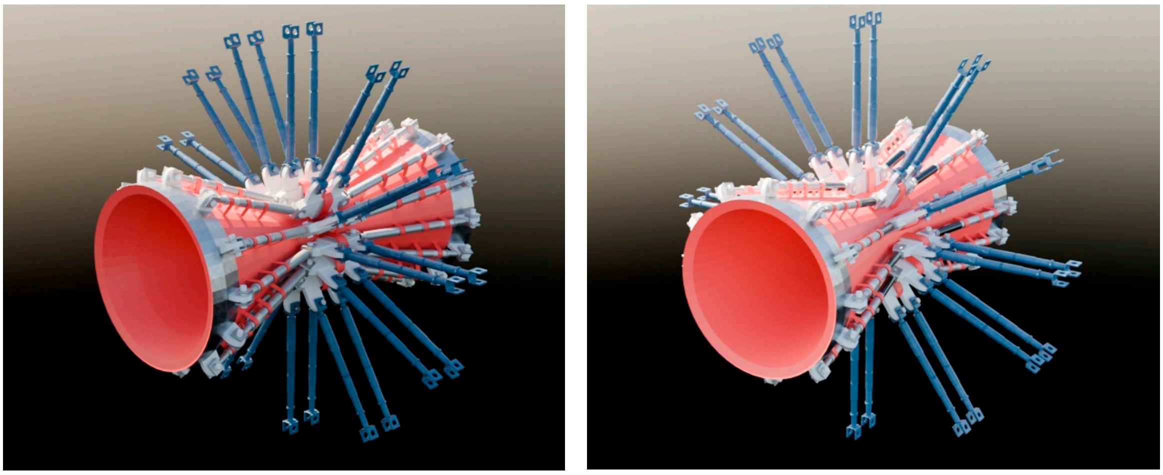

(**a**) (**b**)

Figure 1. Schematic DCVA-S in the two limiting configurations, full Venturi view: (**a**) minimum equivalent throat diameter, $d_e = d$; (**b**) maximum equivalent throat diameter, $d_e = D$. Blue pistons represent the external actuation, white/gray pistons form the kinematic cage, and the red elastomeric liner forms the internal wetted surface.

 doi:10.20944/preprints202602.1423.v1

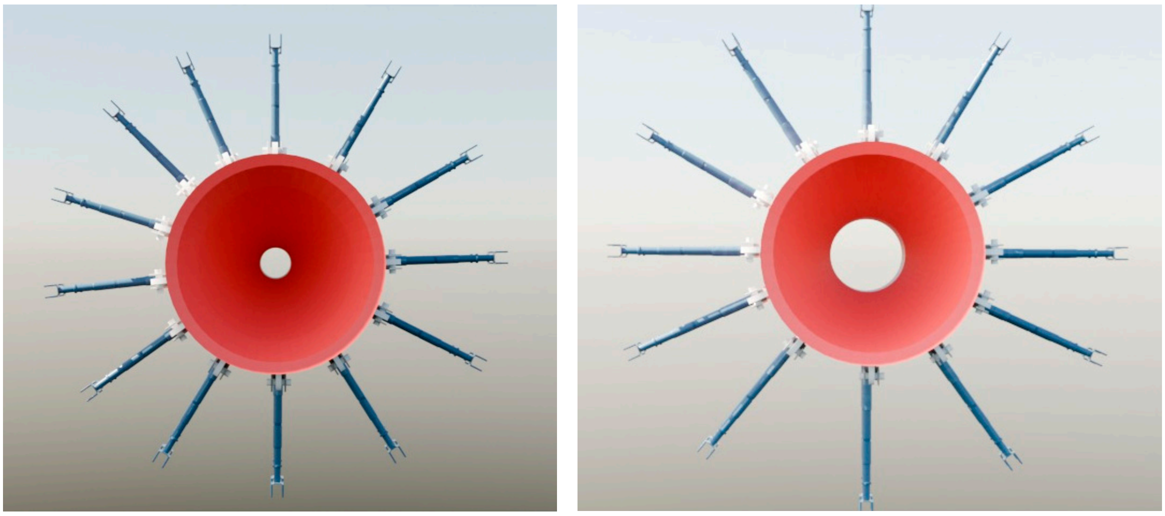

(a) (b)

Figure 2. Schematic front view of the DCVA-S in the two limiting configurations: (**a**) minimum internal throat section, $d_e = d$; (**b**) maximum internal throat section, $d_e = D$. The external interfaces remain unchanged, while the internal geometry varies.

To clarify the modular nature of the kinematic cage, Figure 3 shows the elementary module repeated N_θ times along the circumference.

Let N_θ denote the number of elementary cage modules distributed around the circumference. Increasing N_θ improves the uniformity of the circumferential constraint and, consequently, the repeatability of the resulting internal geometry. Higher values of N_θ reduce local deformations between adjacent constraint points and distribute stresses on the liner more uniformly, at the expense of increased mechanical complexity and more demanding assembly/actuation.

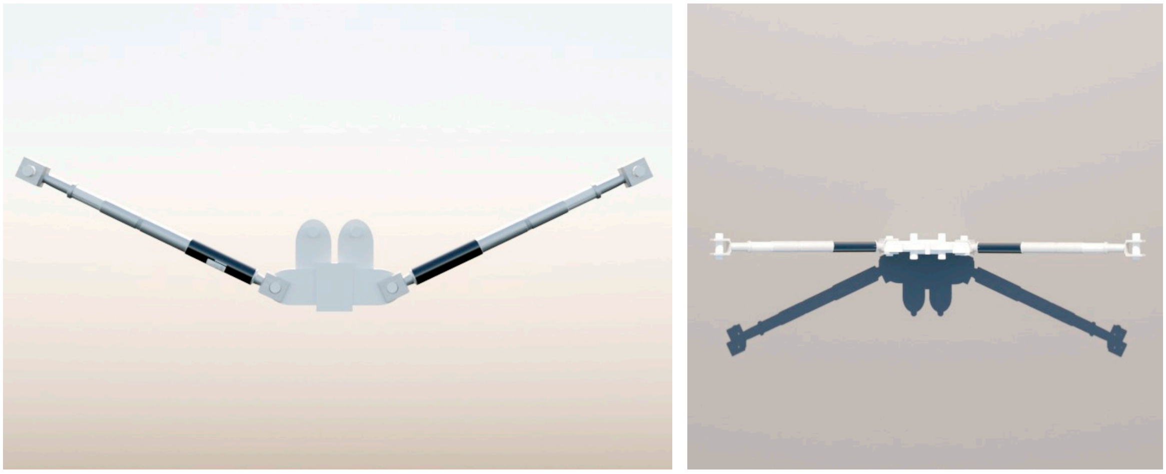

(a) (b)

Figure 3. Schematic elementary module of the DCVA-S kinematic cage: (**a**) front view; (**b**) top view. The module integrates two linear cage actuators (white pistons) connected to a central body through joints. The upper lugs provide the interface points to the external actuators (blue pistons, not shown). The circumferential repetition of N_θ identical modules forms the complete kinematic cage.

The longitudinal section in Figure 4 highlights the continuity of the internal surface and the transfer of motion to the liner.

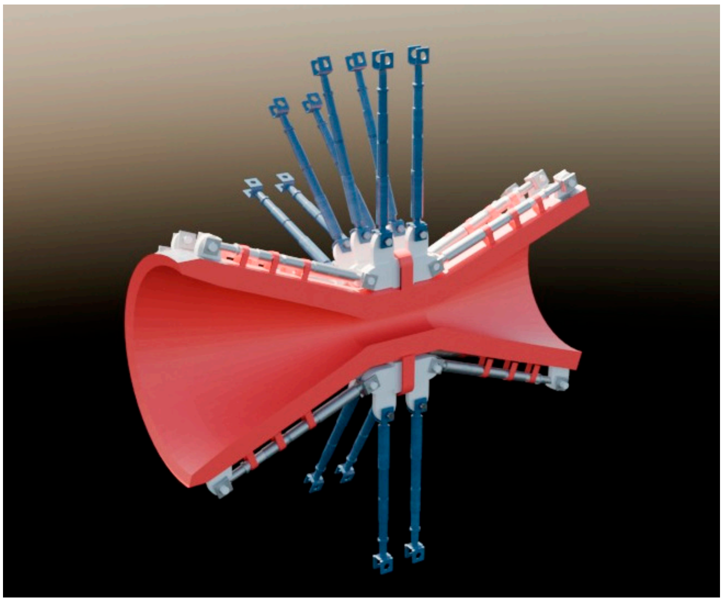

Figure 4. Schematic Longitudinal section of the DCVA-S: the red elastomeric liner, constrained to the white/gray kinematic cage by rings, ensures continuity of the internal surface. Actuation varies d_e, while L_t remains constant due to a mechanical constraint.

3.2. Operation and Kinematics

The reconfiguration of the DCVA-S is described by a single dimensionless parameter $\chi(t) \in [0,1]$, defined within the general framework of Section 2. The control input χ determines the equivalent throat diameter $d_e(t)$ through the control-to-geometry relation reported in Equation (3).

Consistently with Figures 1–4, operation can be summarized as follows. The blue pistons, actuated in a coordinated manner, impose the displacement of the kinematic cage. The cage modules transfer this displacement to the retaining rings. The red liner deforms while maintaining a continuous internal surface, as shown in Figure 4, thereby varying d_e between d and D, as shown in Figures 1 and 2. The inlet and outlet piping interfaces remain unchanged.

In the DCVA-S, the only actuated degree of freedom is the equivalent throat diameter $d_e(\chi)$. The equivalent length of the throat region, L_t, is fixed by design, whereas the effective angles α_{in} and α_{out} vary in a coupled manner with χ and are determined by the kinematics, since they are not independent control variables. The dependencies $\alpha_{in}(\chi)$ and $\alpha_{out}(\chi)$ can be obtained through geometric or experimental calibration and checked against design limits.

Formally, the DCVA-S explores a one-dimensional subset of the design space Ω, parameterized solely by the equivalent throat diameter:

$$\Omega_S = \left\{ (d_e, L_t, \alpha_{in}, \alpha_{out}) \;\middle|\; \begin{array}{c} d \le d_e \le D \\ L_t = \bar{L}_t \\ \alpha_{in} = \alpha_{in}(d_e) \\ \alpha_{out} = \alpha_{out}(d_e) \end{array} \right\} \tag{8}$$

In Equation (8), $\bar{L}_t$ denotes the design value of the equivalent length of the throat region, whereas $\alpha_{in}(d_e)$ and $\alpha_{out}(d_e)$ represent the effective angles induced by the kinematics as d_e varies and can be determined through geometric or experimental calibration.

3.3. Commissioning and Operation

At a conceptual level, the DCVA-S can be operated through a calibration map that links the control input χ to the internal geometry and to the expected cavitation regime. A commissioning map can be constructed by sampling a discrete set of $\chi \in [0,1]$ values and determining the equivalent throat diameter $d_e(\chi)$ via the control-to-geometry relation in Equation (3), with

Preprints.org (www.preprints.org) | NOT PEER-REVIEWED | Posted: 24 February 2026 doi:10.20944/preprints202602.1423.v1

experimental verification when needed. In the same step, the coupled variation of the effective angles imposed by the kinematics is characterized and checked against the design limits. Using available measurements together with Equations (6) and (7), the operational proxy $\hat{\sigma}(\chi)$ is then estimated and a $\hat{\sigma}$–χ curve or lookup table is constructed.

It is emphasized that $\hat{\sigma}$ is an operational proxy computed from p_{in} and the equivalent throat diameter d_e through the velocity estimate v_t; it therefore does not represent a direct measurement of the local cavitation number σ at the throat. During operation, χ is selected as a process control variable to achieve the desired cavitation level, for example within a target range of $\hat{\sigma}$, while satisfying practical plant constraints such as the maximum allowable pressure drop and the mechanical limits of the actuation system.

4. DCVA-M: Multiparametric

The DCVA-M configuration extends the dynamic circular Venturi concept by introducing a multiparametric reconfiguration of the internal profile. The key principle is that the wetted surface is not reconfigured through a single global actuation, but rather through axial stations distributed along the converging section, the throat region, and the diverging section. This architecture generates a family of internal profiles that vary along the axis and enables modulation of the equivalent throat diameter, the shape of the transitions, and the extent of the throat region, while keeping the inlet and outlet piping interfaces unchanged.

4.1. Architecture Multi

The DCVA-M retains an outer cartridge with fixed inlet and outlet connection diameters. Reconfiguration of the internal surface is achieved through axially distributed actuation stations along the Venturi axis. Each station locally sets the radial position of the liner and, through coordinated actuation, generates a family of internal profiles. The color coding of the elements in the figures is kept consistent, with the outer cartridge in green, the liner in red, the actuators in blue, and the kinematic components in white/gray. The external connections remain unchanged, whereas the internal geometry becomes a function of the station commands and can be summarized by the equivalent parameters d_e, L_t, α_{in}, and α_{out}.

Station number and spacing set the profile resolution, while actuation and synchronous coordination are implementation-dependent within this framework.

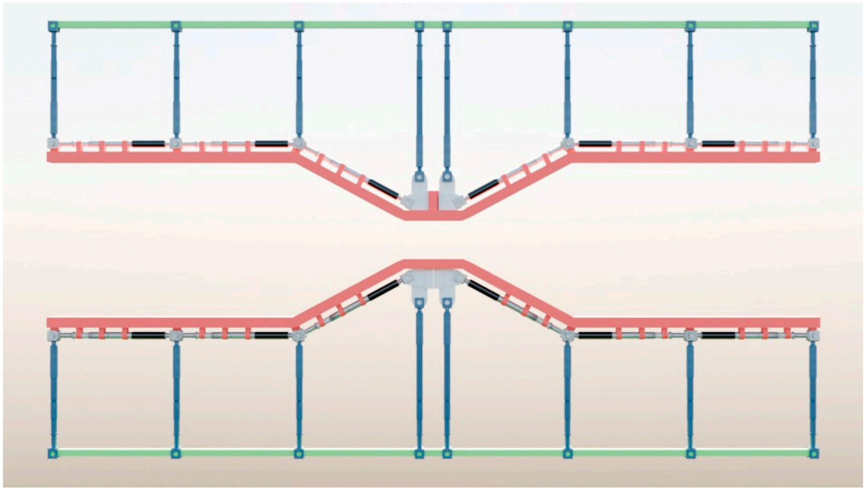

Figure 5. Longitudinal schematic of the DCVA-M with axially distributed actuation. The red liner forms the internal wetted surface. The blue actuators operate across multiple axial actuation stations, while the white/gray components transfer the displacement to the liner through distributed constraints. This enables a

Preprints.org (www.preprints.org) | NOT PEER-REVIEWED | Posted: 24 February 2026 doi:10.20944/preprints202602.1423.v1

multiparametric reconfiguration of the internal profile while keeping the inlet and outlet piping interfaces unchanged.

4.2. Operation and Parameters

In the DCVA-M, reconfiguration is described by a set of dimensionless control inputs associated with the axial actuation stations. The axial layout is defined by the station locations x_i along the Venturi axis, with $i = 1, \dots, N$. The input of station i is denoted by $u_i(t) \in [0,1]$, with $i = 1, \dots, N$. The admissible set of control inputs is defined as

$$\mathcal{U} = \left\{ u \,\middle|\, \begin{array}{c} u = [u_1, \dots, u_N]^T \\ u_i \in [0,1], i = 1, \dots, N \end{array} \right\} \tag{9}$$

In the following, $u(t) \in \mathcal{U}$ is assumed.

The resulting internal profile depends on the control vector u and defines a family of geometries achievable as u varies. Equivalent geometric parameters are introduced to summarize this family. The equivalent throat diameter $d_e(u)$ is defined as the minimum value of the internal profile. The equivalent length of the throat region $L_t(u)$ is defined as the axial extent of the portion close to the minimum according to an operational threshold. The effective inlet and outlet angles, $\alpha_{in}(u)$ and $\alpha_{out}(u)$, are determined as equivalent slopes of the converging and diverging sections through geometric or experimental calibration.

Schematic examples of internal profiles obtained by varying the station control inputs are shown in Figure 6. The figure highlights that multiparametric reconfiguration enables variation not only of d_e, but also of the transition shapes and the extent of the throat region, thereby generating different combinations of d_e, L_t, α_{in}, and α_{out} within the design constraints.

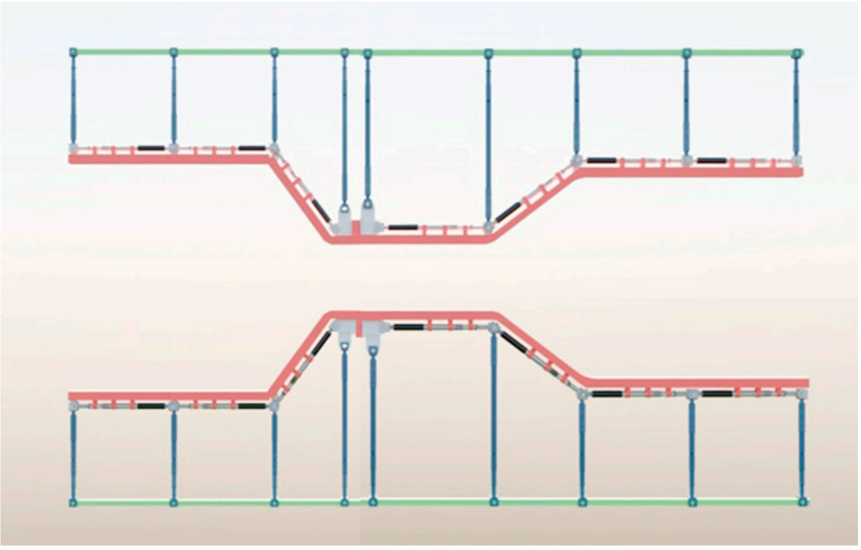

Figure 6. Schematic examples of internal profiles obtained by varying the station control inputs. The profiles are illustrative, not extracted from simulations or experiments, and show how multiparametric reconfiguration can vary d_e, transition shapes, and throat extent, generating different combinations of d_e, L_t, α_{in}, and α_{out} within design constraints.

4.3. Design Space

The DCVA-M realizes only a subset of the admissible geometries in the design space Ω defined in Equation (5), since the kinematics and actuator limits impose constraints on the reachable configurations. In compact form, the set of achievable configurations is described as:

 doi:10.20944/preprints202602.1423.v1

$$\Omega_M = \left\{ (d_e, L_t, \alpha_{in}, \alpha_{out}) \in \Omega \;\middle|\; \exists u \in \mathcal{U}: \begin{array}{l} d_e = d_e(u) \\ L_t = L_t(u) \\ \alpha_{in} = \alpha_{in}(u) \\ \alpha_{out} = \alpha_{out}(u) \end{array} \right\} \quad (10)$$

The functions $d_e(u)$, $L_t(u)$, $\alpha_{in}(u)$, and $\alpha_{out}(u)$ capture the effect of the multiparametric reconfiguration enforced by the axially distributed actuation stations and are determined by the device kinematics and calibration. These equivalent parameters are generally not independent. They are coupled through the kinematics and must remain within mechanical and geometric limits. Ensuring axial smoothness of the control inputs u_i is therefore important to prevent overly segmented profiles and to mitigate localized deformation in the liner. Such smoothness can be enforced during calibration and through the selection of admissible operating configurations.

4.4. Calibration and Operation

At a conceptual level, the DCVA-M can be operated through a calibration procedure that associates representative configurations $u^{(m)} \in \mathcal{U}$ with equivalent internal profiles and expected cavitation levels. Calibration consists of defining a finite set of operating configurations, each characterized by the equivalent values $d_e(u^{(m)})$, $L_t(u^{(m)})$, $\alpha_{in}(u^{(m)})$, and $\alpha_{out}(u^{(m)})$.

A straightforward operating strategy is to build a catalog of profiles. For each configuration, an expected value of the operational proxy $\hat{\sigma}$ can also be estimated using Equations (6) and (7), based on the equivalent throat diameter of the selected profile and the available measurements. In the multiparametric case as well, $\hat{\sigma}$ is used as an operational proxy based on p_{in} and d_e, and it does not replace a direct measurement of local cavitation at the throat.

During operation, the operator or the supervisory system selects a configuration $u \in \mathcal{U}$ from the catalog to achieve the desired cavitation range, while simultaneously satisfying practical plant constraints and the mechanical limits of reconfiguration.

5. Discussion

This A conventional Venturi operates with a fixed geometry and, for given plant conditions, imposes a cavitating operating point that is essentially determined by the throat section. The DCVA introduces a geometric operating variable, since the equivalent throat diameter d_e can be adjusted during operation. For a given flow rate and pressure conditions, varying d_e changes the characteristic throat velocity and allows the cavitation regime to be shifted within a target operating window without altering the external connections.

This aspect is particularly relevant for complex liquids, for which the properties of the process fluid and operating conditions may vary over time. In such cases, a fixed geometry sized for a single operating point may be suboptimal or insufficiently robust. Within the proposed framework, internal reconfiguration decouples plant integration, which remains unchanged, from cavitation-regime control, which becomes adaptable.

In follow-up work, commissioning maps will be extended by parameterizing operating settings versus T and relevant fluid properties, and by incorporating thermo-cavitation and suppression mechanisms reported for Venturi devices when required by the specific duty.

Introducing the design space Ω makes it possible to distinguish between the set of admissible geometries and the subset that is actually reachable for a given architecture. In the DCVA-S, exploration is essentially one-dimensional, because the directly actuated degree of freedom is d_e, whereas the equivalent throat-region length and the effective angles are fixed or induced by the kinematics.

In the DCVA-M, reconfiguration is driven by a set of station control inputs belonging to $\mathcal{U}$ and generates a family of internal profiles. Consequently, the equivalent parameters d_e, L_t, α_{in}, and α_{out} vary in a coupled manner as functions of the control input. From this perspective, DCVA-S prioritizes simplicity and repeatability, whereas DCVA-M expands the effectively explorable geometric space at the cost of more articulated kinematic constraints and calibration requirements.

The choice between DCVA-S and DCVA-M can be formulated as a trade-off between geometric flexibility and overall complexity. DCVA-S enables direct modulation of cavitation intensity through d_e with a single control input, making calibration-map-based operation straightforward and keeping the device conceptually simple.

DCVA-M, in contrast, enables adjustment not only of d_e but also of the transition shapes and the extent of the throat region. These aspects influence the pressure-field distribution, flow stability, and the spatial localization of cavitation. In this regard, numerical studies combining cavitation modelling with turbulence closures show that model choices can significantly affect predicted cavitation structures and unsteadiness, which is relevant when assessing the effects of profile reconfiguration. Recent reviews further summarize advances and remaining challenges in cavitation prediction and suppression, providing context for interpreting shifts in cavitation localization and stability induced by geometry changes. This added capability, however, requires a more rigorous definition of admissible configurations, a more extensive calibration procedure, and more careful operational management.

In this work, $\hat{\sigma}$ is used as an operational proxy to link plant-measurable quantities to the equivalent device geometry through d_e. The proxy supports calibration-map construction, configuration comparisons, and the selection of operating settings under a consistent estimation criterion. At the same time, $\hat{\sigma}$ does not replace a direct measurement of the local cavitation number at the throat and should be interpreted in light of the assumptions behind the velocity estimate and the presence of distributed losses.

For engineering reproducibility, the DCVA concepts are specified through the key geometric and kinematic parameters summarized in Table 1; application-specific dimensions and material choices are not prescribed in this sector-agnostic framework, and repeatability is addressed during commissioning by measuring the relevant geometry mappings.

Adopting the DCVA also introduces constraints that affect both design and operation. The repeatability of the equivalent geometry may be influenced by hysteresis and mechanical tolerances, while liner durability depends on stress distribution and cyclic deformation. Accordingly, material selection can draw on recent developments in sustainable elastomers and durability-oriented design approaches, on EPDM-based compatibilization strategies to improve low-temperature robustness, and on nano-carbon reinforcement routes for high-performance elastomers under cyclic loading.

The DCVA can be used as a reusable tool to explore and identify the optimal cavitation operating window in a given application, for example in food processing to maximize a target extraction, and then be moved to a different context such as water treatment to optimize the removal of a specific pollutant; once the optimal window is identified, a dedicated static Venturi can be manufactured for continuous operation.

Accordingly, the DCVA is benchmarked in follow-up work through system-level metrics rather than performance claims, including the achievable regime-modulation range with unchanged in-line interfaces, the commissioning effort to identify a robust operating window, and the transfer from exploratory tuning to a finalized static Venturi for continuous duty.

Although the present study is conceptual and does not report a complete experimental validation, deployment in process plants can be supported by essential verification steps. These include calibrating the control-to-geometry relationship to obtain d_e and, when relevant, the other equivalent parameters; constructing control–$\hat{\sigma}$ maps under nominal conditions; verifying the operating window in terms of pressure drop; and qualitatively correlating variations in $\hat{\sigma}$ with independent cavitation indicators to support proxy interpretation.

 doi:10.20944/preprints202602.1423.v1

6. Conclusions

This work presents a conceptual system design framework for the Dynamic Circular Venturi (DCVA), a reconfigurable circular Venturi conceived as a drop-in in-line replacement. The device preserves the external body and the inlet and outlet piping interfaces while making the internal throat configuration a design and operating degree of freedom. A formalism based on equivalent geometric parameters and a dedicated design space is defined, and two representative architectures are described, namely a single degree-of-freedom configuration and a multiparametric configuration. An operational proxy indicator is also introduced, computable from quantities typically available in process plants, to support configuration selection and unambiguous specification of operating settings when local throat pressure is not directly accessible. No experimental campaign or high-fidelity CFD results are reported, as the present contribution is intended as a conceptual design framework rather than a performance-validation study.

The proposed framework is directly relevant to sustainable food-processing duties where hydrodynamic cavitation is used as a green process-intensification route, because controllable throat modulation can support robust operation, resource-efficiency improvements, and waste minimization.

Quantitative evidence will be generated in follow-up work for a selected industrial duty by measuring the command–geometry mappings and their repeatability under cycling, constructing commissioning maps linking configuration and plant conditions to cavitation indicators and process targets while verifying pressure-drop constraints, and correlating $\hat{\sigma}$ and configuration changes with independent cavitation diagnostics and process outcomes. When required by the duty, numerical analysis can be used to support interpretation under specified boundary conditions.

Funding: This research received no external funding.

Data Availability Statement: The original contributions presented in this study are included in the article. Further inquiries can be directed to the corresponding author.

Conflicts of Interest: The author declares no conflicts of interest.

Abbreviations

The following abbreviations are used in this manuscript:

DCVA	Dynamic Circular Venturi
DCVA-S	Dynamic Circular Venturi Single-parameter
DCVA-M	Dynamic Circular Venturi Multiparametric

References

1. A Panda, D.; Saharan, V.K.; Manickam, S. Controlled Hydrodynamic Cavitation: A Review of Recent Advances and Perspectives for Greener Processing. Processes **2020**, 8, 220. https://doi.org/10.3390/pr8020220.
2. Carpenter, J.; Badve, M.; Rajoriya, S.; Pandit, A.B. Hydrodynamic Cavitation: An Emerging Technology for the Intensification of Various Chemical and Physical Processes in a Chemical Process Industry. *Rev. Chem. Eng.* **2017**, 33, 433–468. https://doi.org/10.1515/revce-2016-0032.
3. Arya, S.S.; More, P.R.; Ladole, M.R.; Pegu, K.; Pandit, A.B. Non-thermal, Energy Efficient Hydrodynamic Cavitation for Food Processing, Process Intensification and Extraction of Natural Bioactives: A Review. *Ultrason. Sonochem.* **2023**, 98, 106504. https://doi.org/10.1016/j.ultsonch.2023.106504.
4. Zoglopiti, E.; Roufou, S.; Psakis, G.; Okafor, E.T.; Dasenaki, M.; Gatt, R.; Valdramidis, V.P. Unravelling the Hydrodynamic Cavitation Potential in Food Processing: Underlying Mechanisms, Crucial Parameters, and Antimicrobial Efficacy. *Food Eng. Rev.* **2025**. https://doi.org/10.1007/s12393-025-09419-4.
5. Wu, Z.; Ferreira, D.F.; Crudo, D.; Bosco, V.; Stevanato, L.; Costale, A.; Cravotto, G. Plant and Biomass Extraction and Valorisation under Hydrodynamic Cavitation. *Processes* **2019**, 7, 965. https://doi.org/10.3390/pr7120965.

6. Petkovšek, M.; Zupanc, M.; Dular, M.; Kosjek, T.; Heath, E.; Kompare, B.; Širok, B. Rotation Generator of Hydrodynamic Cavitation for Water Treatment. *Sep. Purif. Technol.* **2013**, 118, 415–423. https://doi.org/10.1016/j.seppur.2013.07.029.
7. Viswanathan, S. Development of a Pressure Drop Model for a Variable Throat Venturi Scrubber. *Chem. Eng. J.* **1998**, 71, 153–160. https://doi.org/10.1016/S1385-8947(98)00123-5.
8. Brady, J.D.; Legatski, L.K. Variable Throat Venturi Scrubber. U.S. Patent US4023942A, **1977**.
9. Tian, H.; Zeng, P.; Yu, N.; Cai, G. Application of Variable Area Cavitating Venturi as a Dynamic Flow Controller. *Flow Meas. Instrum.* **2014**, 38, 21–26. https://doi.org/10.1016/j.flowmeasinst.2014.05.012.
10. Tan, G.; Tian, H.; Gu, X.; Meng, X.; Wei, T.; Zhang, Y.; Cai, G. Flow Feedback Control Based on Variable Area Cavitating Venturi and Its Application in Hybrid Rocket Motors. *Acta Astronaut.* **2023**, 211, 238–248. https://doi.org/10.1016/j.actaastro.2023.06.013.
11. Long, X.; Sun, M.; Chen, L.; et al. Research on Cavitation and Oscillation Transition Mechanism of Adjustable Cavitation Venturi Tube. *J. Hydrodyn.* **2025**, 37, 680–697. https://doi.org/10.1007/s42241-025-0050-1.
12. Albanese, L.; Centritto, M.; Meneguzzo, F. Apparatus for Dynamically Regulating Hydrodynamic Cavitation Processes and Related Process. European Patent EP4260934A1, **2023**.
13. Simpson, A.; Ranade, V.V. Modeling Hydrodynamic Cavitation in Venturi: Influence of Venturi Configuration on Inception and Extent of Cavitation. *AIChE J.* **2019**, 65, 421–433. https://doi.org/10.1002/aic.16411.
14. Brennen, C.E. *Cavitation and Bubble Dynamics*; Oxford University Press: Oxford, UK, **1995**. https://doi.org/10.1093/oso/9780195094091.001.0001.
15. Franc, J.-P.; Michel, J.-M. *Fundamentals of Cavitation*; Kluwer Academic Publishers: Dordrecht, The Netherlands, **2004**. https://doi.org/10.1007/1-4020-2233-6.
16. Rütten, E.; Leister, N.; Karbstein, H.P.; Håkansson, A. Possibilities and Limits of Modeling Cavitation in High-Pressure Homogenizers—A Validation Study. *Chem. Eng. Sci.* **2024**, 283, 119405. https://doi.org/10.1016/j.ces.2023.119405.
17. Tan, G.; Tian, H.; Lv, G. Experimental Study on Flow Coefficient of Variable Area Cavitating Venturi. In *Proceedings of the 8th International Conference on Manufacturing, Material and Metallurgical Engineering (ICMMME 2024)*; Agarwal, R.K., Ed.; Lecture Notes in Mechanical Engineering; Springer: Cham, Switzerland, **2025**. https://doi.org/10.1007/978-3-031-78295-4_14.
18. ISO. ISO 37:2017. Rubber, Vulcanized or Thermoplastic—Determination of Tensile Stress–Strain Properties; International Organization for Standardization: Geneva, Switzerland, **2017**.
19. Wang, G.; Senocak, I.; Shyy, W.; Ikohagi, T.; Cao, S. Dynamics of Attached Turbulent Cavitating Flows. *Prog. Aerosp. Sci.* **2001**, 37, 551–581. https://doi.org/10.1016/S0376-0421(01)00014-8.
20. Lee, H.; Lee, C.; Kim, M.-S.; Seok, W. Numerical Investigation of Cavitation Models Combined with RANS and PANS Turbulence Models for Cavitating Flow Around a Hemispherical Head-Form Body. *J. Mar. Sci. Eng.* **2025**, 13, 821. https://doi.org/10.3390/jmse13040821.
21. Qiu, Q.; Gu, Y.; Ren, Y.; Mou, C.; Hu, C.; Ding, H.; Wu, D.; Wu, Z.; Mou, J. Research Progress in Hydrofoil Cavitation Prediction and Suppression Methods. *Phys. Fluids* **2025**, 37, 011301. https://doi.org/10.1063/5.0245462.
22. Filippova, O.V.; Maksimkin, A.V.; Dayyoub, T.; Larionov, D.I.; Telyshev, D.V. Sustainable Elastomers for Actuators: "Green" Synthetic Approaches and Material Properties. *Polymers* **2023**, 15, 2755. https://doi.org/10.3390/polym15122755.
23. Liu, G.; Du, F.; Yao, Z.; Li, G.; Kuang, W.; Zhu, C.; Liu, Y.; Chen, H.; Wang, F.; Zhou, C.; et al. Effects of Ethylene Propylene Diene Monomer (EPDM)-Based Polar Macromolecular Compatibilizers on the Low-Temperature Properties of Fluoroelastomer/EPDM Rubber Blends. *Molecules* **2024**, 29, 5522. https://doi.org/10.3390/molecules29235522.
24. Valentini, L.; López-Manchado, M.A., Eds. *High-Performance Elastomeric Materials Reinforced by Nano-Carbons: Multifunctional Properties and Industrial Applications*; Elsevier: Amsterdam, The Netherlands, **2020**; ISBN 978-0-12-816198-2. https://doi.org/10.1016/C2017-0-04735-3.

doi:10.20944/preprints202602.1423.v1

25. Zheng, H.; Zheng, Y.; Zhu, J. Recent Developments in Hydrodynamic Cavitation Reactors: Cavitation Mechanism, Reactor Design, and Applications. Engineering 2022, 19, 180–198. https://doi.org/10.1016/j.eng.2022.04.027.
26. Ghassemi, H.; Farshi Fasih, H. Application of small size cavitating venturi as flow controller and flow meter. Flow Measurement and Instrumentation 2011, 22, 406–412. https://doi.org/10.1016/j.flowmeasinst.2011.05.001.
27. Mena, J. L.; Ingle, M. A.; Shirsat, V.; Choudhuri, A. An investigation of a cavitating venturi flow control feature in a cryogenic propellant delivery system. Flow Measurement and Instrumentation 2015, 41, 97–103. https://doi.org/10.1016/j.flowmeasinst.2014.09.008.
28. Ashrafizadeh, S. M.; Ghassemi, H. Experimental and numerical investigation on the performance of small-sized cavitating venturis. Flow Measurement and Instrumentation 2015, 42, 6–15. https://doi.org/10.1016/j.flowmeasinst.2014.12.007.
29. Ge, M.; Petkovšek, M.; Zhang, G.; Jacobs, D.; Coutier-Delgosha, O. Cavitation Dynamics and Thermodynamic Effects at Elevated Temperatures in a Small Venturi Channel. Int. J. Heat Mass Transf. 2021, 170, 120970. https://doi.org/10.1016/j.ijheatmasstransfer.2021.120970.
30. Ge, M.; Sun, C.; Zhang, G.; Coutier-Delgosha, O.; Fan, D. Combined Suppression Effects on Hydrodynamic Cavitation Performance in Venturi-Type Reactor for Process Intensification. Ultrason. Sonochem. 2022, 86, 106035. https://doi.org/10.1016/j.ultsonch.2022.106035.